Systematic analysis of nucleon scattering from ^{6,7}Li with the continuum discretized coupled channels method

Hairui Guo,[1,*] Yukinobu Watanabe,[1] Takuma Matsumoto,[2] Kazuyuki Ogata,[3] and Masanobu Yahiro[2]
[1]*Department of Advanced Energy Engineering Science, Kyushu University, Kasuga, Fukuoka 816-8580, Japan*
[2]*Department of Physics, Kyushu University, Fukuoka 812-8581, Japan*
[3]*Research Center for Nuclear Physics, Osaka University, Ibaraki, Osaka 567-0047, Japan*
(Received 17 December 2012; revised manuscript received 21 January 2013; published 25 February 2013)

Nucleon scattering from ^{6,7}Li is analyzed systematically over a wide range of incident energies up to 150 MeV with the continuum discretized coupled channels method (CDCC) capable of treating the breakup of ^{6,7}Li. The continuum states of ^{6,7}Li are discretized with the pseudostate method. Diagonal and coupling potentials in the CDCC equation are obtained by folding the complex Jeukenne-Lejeune-Mahaux effective nucleon-nucleon interaction with transition densities between corresponding bound and discretized continuum states of ^{6,7}Li. The normalization factors of the complex effective interaction are determined so as to reproduce experimental data on neutron total and proton reaction cross sections for ^{6,7}Li. CDCC calculations with the normalization factors reproduce experimental differential cross sections for nucleon elastic and inelastic scattering from ^{6,7}Li well.

DOI: 10.1103/PhysRevC.87.024610 PACS number(s): 25.40.−h, 24.10.Eq, 25.60.Gc

I. INTRODUCTION

Lithium isotopes ^{6,7}Li are important tritium breeding materials in deuterium-tritium (D-T) fusion reactors. The tritium breeding ratio, nuclear heating distribution, and radiation damage of structural materials are affected significantly by the interaction between neutrons and lithium nuclei in fusion reactor blankets. Moreover, liquid lithium is a candidate for target material in the intense neutron source of International Fusion Materials Irradiation Facility (IFMIF) [1]. Accurate nuclear data are therefore required for nucleon induced reactions on ^{6,7}Li at incident energies up to 150 MeV [2]. In addition, ^{6}Li and ^{7}Li are weakly bound nuclei, which can easily break up into two fragments, namely, $^{6}\mathrm{Li} \to d + \alpha$ and $^{7}\mathrm{Li} \to t + \alpha$. The breakup process is, therefore, important for nucleon induced reactions on ^{6,7}Li. Systematic understanding of the breakup mechanism is also an interesting and meaningful subject from the viewpoint of nuclear physics. Study of nucleon-induced reactions on ^{6,7}Li targets is thus not only of application value but also of theoretical significance.

The continuum discretized coupled channels method (CDCC) [3,4] has so far been applied successfully to many studies on breakup processes of weakly bound light nuclei [3–10], which includes studies of projectile breakup reactions of ^{6,7}Li interacting with some medium and heavy target nuclei. Elastic and inelastic scattering of ^{6,7}Li have been analyzed for various targets ranging from ^{12}C to ^{208}Pb with CDCC [3] in which the real parts of the diagonal and coupling potentials are obtained by folding the M3Y nucleon-nucleon (NN) interaction and the imaginary parts are assumed to have the same shape as the real part. Intensive studies [9,10] on ^{6,7}Li interactions with ^{208}Pb near the Coulomb barrier have also been made with CDCC in order to explain the radiative capture nucleosynthesis process in nuclear astrophysics.

With regard to nucleon-induced reactions on ^{6,7}Li, Ichinkhorloo *et al.* have analyzed $n + {}^{6}$Li reaction for incident energies from 7.47 to 24.0 MeV by using CDCC with phenomenological proton optical potentials. However, the agreement of the elastic cross sections at all the incident neutron energies is insufficient because of the lack of information on the optical potentials for n-d and n-α subsystems [11]. Matsumoto *et al.* [12] have investigated $^{6}\mathrm{Li}(n, n')^{6}\mathrm{Li}^{*} \to d + \alpha$ reaction for incident energies below 24 MeV by using CDCC with the complex Jeukenne-Lejeune-Mahaux (JLM) effective nucleon-nucleon (NN) interaction [13]. They have found that the CDCC calculation can reproduce well measured angular distributions of neutron elastic and inelastic scattering from ^{6}Li and double differential $(n, \mathrm{x}n)$ cross sections at relatively high emission energies. In their analysis of total cross sections for $n + {}^{6}$Li reaction, it was suggested that an energy-dependent trend appears in the normalization factors of the JLM interaction as the incident energy increases. More recently, Ichinkhorloo *et al.* [14] have analyzed $n + {}^{7}$Li scattering for incident energies below 24 MeV by using CDCC with the JLM NN interaction. Their CDCC calculation reproduces experimental angular distributions for neutron elastic and inelastic scattering from ^{7}Li and double differential $(n, \mathrm{x}n)$ cross sections at relatively high emission energies for incident energies between 11.5 and 24.0 MeV.

In the present work, therefore, we extend CDCC analysis of Refs. [12,14] to both neutrons and protons scattering from ^{6,7}Li in a wide incident energy range up to 150 MeV, and demonstrate the applicability of CDCC to nucleon scattering from ^{6,7}Li.

We analyze neutron total cross sections, proton reaction cross sections, and differential cross sections for nucleon elastic and inelastic scattering. ^{6}Li and ^{7}Li are considered as $d + \alpha$ and $t + \alpha$ cluster, respectively. Continuum states of ^{6}Li and ^{7}Li are discretized by the pseudostate method [15,16]. Diagonal and coupling potentials in the CDCC equation are obtained by folding the JLM effective

*ghr@aees.kyushu-u.ac.jp

NN interaction with the transition densities between corresponding bound and discretized continuum states of ^{6,7}Li. The normalization factors of the JLM effective NN interaction are determined so as to reproduce experimental data on the neutron total cross sections and proton reaction cross sections. CDCC yields consistent results with experimental data on the angular distributions for nucleon elastic and inelastic scattering.

Section II describes the theoretical model. In Sec. III, CDCC results are compared with experimental data. Finally, Sec. IV gives a summary and conclusions.

II. THEORETICAL MODEL

Nucleon scattering from ^{6,7}Li is analyzed with the $N_0 + x + \alpha$ three-body model, where N_0 denotes an incident nucleon and x represents deuteron (d) for ^{6}Li and triton (t) for ^{7}Li.

A. Bound- and discretized-state wave functions of ^{6,7}Li

We assume that the wave functions of ^{6}Li and ^{7}Li are expressed as

$$\Phi_l^{Im}(\boldsymbol{\xi}) = \psi_l^{Im}(\boldsymbol{r})\varphi(x)\varphi(\alpha), \tag{1}$$

where $\boldsymbol{\xi}$ represents a set of internal coordinates of Li. $\varphi(x)$ and $\varphi(\alpha)$ denote the internal wave functions of x and α, respectively, which are assumed to be inert cores. $\varphi(x)$ does not include a spin degree of freedom. $\psi_l^{Im}(\boldsymbol{r})$ is the x-α relative wave function with relative coordinate $\boldsymbol{r}$, orbital angular momentum l, total spin I and its projection m on the z axis, which is defined as

$$\psi_l^{Im}(\boldsymbol{r}) = \phi_l^I(r)[i^l Y_l(\Omega_r) \otimes \eta_x]_{Im}, \tag{2}$$

with η_x denoting the spin wave function of x. The relative Hamiltonian between x and α is described by

$$H_{\rm Li} = K_r + V_{x\alpha}(\boldsymbol{r}), \tag{3}$$

where K_r is kinetic energy operator, and $V_{x\alpha}(\boldsymbol{r})$ is the interaction between x and α.

In CDCC calculations, the wave functions of continuum states of ^{6}Li and ^{7}Li are truncated and discretized into a finite number of states. The bound and discretized relative internal wave functions of ^{6}Li and ^{7}Li are then expressed as

$$\hat{\psi}_{nl}^{Im}(\boldsymbol{r}) = \hat{\phi}_{nl}^I(r)[i^l Y_l(\Omega_r) \otimes \eta_x]_{Im}, \ (n = 1, \ldots, N), \tag{4}$$

where l is truncated by $l \leqslant 2$ ($l \leqslant 3$) for ^{6}Li (^{7}Li), and odd (even) l states of ^{6}Li (^{7}Li) are ignored because their contributions are much smaller than those of even (odd) states [3]. N denotes the number of the bound and discretized continuum states for each (l, I).

The pseudostate method [15,16] with the Gaussian expansion of wave function [17] is used to describe the discretized continuum states of ^{6}Li and ^{7}Li. The radial part of the bound and discretized continuum wave functions are then obtained by

$$\hat{\phi}_{nl}^I(r) = \sum_i A_{nl,i}^I \varphi_{il}^{\rm C}(r) + \sum_i B_{nl,i}^I \varphi_{il}^{\rm S}(r) \tag{5}$$

TABLE I. Parameters of the interaction between d and α.

parameters	$l = 0$	$l = 2$
$r_{1,l}$ [fm]	2.191	2.377
$r_{2,l}$ [fm]	1.607	1.852
$v_{1,l}$ [MeV]	− 105.85	− 82.98
$v_{2,l}$ [MeV]	46.22	31.0
$v_{1,l}^{(\rm so)}$ [MeV]	–	− 2.31
$v_{2,l}^{(\rm so)}$ [MeV]	–	1.42
$R_{\rm CL}$ [fm]	3.0	3.0

with the coefficients, $A_{nl,i}^I$ and $B_{nl,i}^I$, determined by diagonalizing $H_{\rm Li}$. Since the highest incident energy considered here is 150 MeV, we need to calculate the discretized continuum states up to a relatively high energy. The complex-range Gaussian basis function [18] is more reliable than the real-range Gaussian basis for describing the breakup states up to a high energy [16]. We then adopt the complex-range Gaussian basis as the basis function. $\varphi_{il}^{\rm C}$ and $\varphi_{il}^{\rm S}$ are the complex-range Gaussian basis functions defined by

$$\begin{aligned} \varphi_{il}^{\rm C}(r) &= [\varphi_{il}^*(r) + \varphi_{il}(r)]/2, \\ \varphi_{il}^{\rm S}(r) &= [\varphi_{il}^*(r) - \varphi_{il}(r)]/(2i), \end{aligned} \tag{6}$$

where

$$\varphi_{il}(r) = r^l \exp\left[-(1 + ib)r^2/a_i^2\right] \tag{7}$$

with $a_1 = 1.0$ fm, $a_N = 20.0$ fm, $b = \pi/2$, and $a_i = a_1(a_N/a_1)^{(i-1)/(N-1)}$. $\hat{\phi}_{nl}^I$ satisfies

$$\left\langle \hat{\phi}_{nl}^I \middle| H_{\rm Li} \middle| \hat{\phi}_{n'l}^I \right\rangle = \epsilon_{nl}^I \delta_{nn'} \tag{8}$$

and

$$\left\langle \hat{\phi}_{nl}^I \middle| \hat{\phi}_{n'l'}^{I'} \right\rangle = \delta_{nn'}\delta_{ll'}\delta_{II'}, \tag{9}$$

where ϵ_{nl}^I is the eigenenergy of the bound or discretized continuum state. The interactions between x and α, $V_{x\alpha}$ in $H_{\rm Li}$, have the same form as in Ref. [3] for both ^{6}Li and ^{7}Li. Here we use a simple version of the orthogonal condition model [3,19], namely, we regard the lowest bound state as the forbidden state and adjust the strength of $V_{x\alpha}$ for the second bound state to reproduce the measured binding energy of Li. Therefore, the parameters of $V_{x\alpha}$, which are listed in Tables I and II, are slightly changed from the original ones.

Figure 1 shows the eigenenergies of the bound and discretized continuum states of ^{6,7}Li for each (l, I) with truncation energy of 10.5 MeV, where the breakup thresholds of ^{6,7}Li are

TABLE II. Parameters of the interaction between t and α.

parameters	$l = 1$	$l = 3$
$r_{1,l}$ [fm]	2.447	2.608
$v_{1,l}$ [MeV]	− 88.11	− 75.38
$r_l^{(\rm so)}$ [fm]	3.6538	2.466
$v_l^{(\rm so)}$ [MeV]	− 6.0	− 2.736
$a_l^{(\rm so)}$ [fm]	0.6	–
$R_{\rm CL}$ [fm]	2.0	2.0

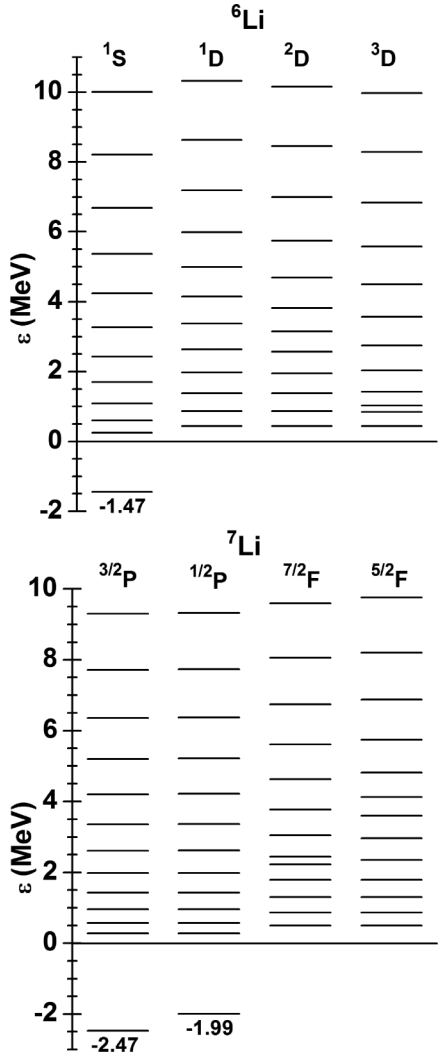

FIG. 1. Eigenenergies of the bound and discretized states of ^{6,7}Li for each (l, I) with truncation energy of 10.5 MeV.

considered as 0 MeV. It is shown that the eigenenergies of the bound states of ^{6,7}Li are described well.

B. Three-body CDCC formulation for nucleon scattering from ^{6,7}Li

The Hamiltonian of the $N_0 + x + \alpha$ three-body system is described by

$$H = H_{\rm Li} + K_R + U_{\rm C}(R) + U, \tag{10}$$

where $\boldsymbol{R}$ represents the relative coordinate between the incident nucleon and the center of mass of Li, and K_R represents the kinetic energy associated with R. The potential between N_0 and a Li target, U, is described as

$$U = \sum_{j\in{\rm Li}} v_{0j} \tag{11}$$

with v_{0j} denoting the interaction between N_0 and the jth nucleon in Li. The Coulomb potential, $U_{\rm C}$, between N_0 and Li is treated approximately as a function of R.

The total wave function of the three-body system with total angular momentum J and its projection M on the z axis can be expanded in terms of the orthonormal set of eigenstates of $H_{\rm Li}$. Using the bound and discretized internal wave functions of ^{6,7}Li obtained in Sec. II A, the total wave function of the three-body system can be expressed as

$$\Psi^{\rm CDCC}_{JM} = \sum_{\gamma} \mathcal{Y}^{lIL}_{JM} \hat{\phi}^{I}_{nl}(r) \hat{\chi}_{\gamma}(\hat{P}_{\gamma}, R)/R, \tag{12}$$

with

$$\mathcal{Y}^{lIL}_{JM} = \{[i^l Y_l(\Omega_r) \otimes \eta_x]_I \otimes i^L Y_L(\Omega_R)\}_{JM} \varphi(x)\varphi(\alpha), \tag{13}$$

where $\gamma = (n, l, I, L, J)$ represents the elastic, inelastic, and breakup channels. The expansion coefficient $\hat{\chi}_{\gamma}$ describes the relative motion between an incident nucleon and Li, and L is the orbital angular momentum. The relative momentum $\hat{P}_{\gamma}$ is determined by the conservation of the total energy,

$$E = \hat{P}^2_{\gamma}/(2\mu) + \epsilon^{I}_{nl}, \tag{14}$$

where μ is the reduced mass of the nucleon-Li system.

In the CDCC formalism, the Schrödinger equation

$$(H - E)\Psi^{\rm CDCC}_{JM} = 0 \tag{15}$$

is rewritten into a set of CDCC differential equations,

$$\left[\frac{d^2}{dR^2} + \hat{P}^2_{\gamma} - \frac{L(L+1)}{R^2} - \frac{2\mu}{\hbar^2} U_{\rm C}(R)\right] \hat{\chi}_{\gamma}(\hat{P}_{\gamma}, R) = \sum_{\gamma'} \frac{2\mu}{\hbar^2} V_{\gamma\gamma'}(R) \hat{\chi}_{\gamma'}(\hat{P}_{\gamma'}, R). \tag{16}$$

Here diagonal ($\gamma' = \gamma$) and coupling ($\gamma' \neq \gamma$) potentials, $V_{\gamma\gamma}$ and $V_{\gamma'\gamma'}$, are obtained as

$$V_{\gamma\gamma'}(R) = \int \rho_{\gamma\gamma'}(\boldsymbol{s}, \Omega_R) v_{0j}(\boldsymbol{r}_{0j}, \bar{\rho}, E) d\boldsymbol{s} d\Omega_R \tag{17}$$

by folding the JLM effective NN interaction v_{0j} [13] with transition densities

$$\rho_{\gamma\gamma'}(\boldsymbol{s}, \Omega_R) = \left\langle \mathcal{Y}^{lIL}_{JM} \hat{\phi}^{I}_{nl} \middle| \sum_{j\in{\rm Li}} \delta(\boldsymbol{s} - \boldsymbol{s}_j) \middle| \mathcal{Y}^{l'I'L'}_{JM} \hat{\phi}^{I'}_{n'l'} \right\rangle, \tag{18}$$

where

$$\bar{\rho}(s) = \frac{1}{2} \int [\rho_{\gamma\gamma}(\boldsymbol{s}, \Omega_R) + \rho_{\gamma'\gamma'}(\boldsymbol{s}, \Omega_R)] d\Omega_s d\Omega_R \tag{19}$$

with $\boldsymbol{r}_{0j}$ ($\boldsymbol{s}_j$) denoting the coordinate of jth nucleon in Li relative to an incident nucleon N_0 (the center of mass of Li). The JLM effective NN interaction v_{0j} is expressed as

$$v_{0j}(\boldsymbol{r}_{0j}, \bar{\rho}, E) = \lambda_V V(\bar{\rho}, E) \exp\left(-\frac{|\boldsymbol{r}_{0j}|^2}{t_R^2}\right) + i\lambda_W W(\bar{\rho}, E) \exp\left(-\frac{|\boldsymbol{r}_{0j}|^2}{t_I^2}\right) \tag{20}$$

with $t_R = t_I = 1.2$ fm. As suggested in Ref. [12], the normalization factors λ_V and λ_W are energy dependent. They are determined so as to reproduce the experimental data on neutron total cross sections and proton reaction cross sections.

C. Compound elastic and inelastic scattering contribution

The Hauser-Feshbach theory with the width fluctuation correction [20] is applied to include the compound elastic and inelastic scattering contribution in the present analysis. The compound nucleus contribution is estimated with TALYS code [21] with the nucleon optical potentials of Koning and Delarosche [22] and the complex-particle optical potentials obtained by folding the nucleon optical potentials. In the calculation, the compound formation cross section is given by

$$\sigma_{\rm CF} = \sigma_{\rm R} - \sigma_{\rm Inel}, \tag{21}$$

where $\sigma_{\rm R}$ and $\sigma_{\rm Inel}$ denote the reaction and inelastic scattering cross sections calculated with CDCC, respectively.

III. CALCULATED RESULTS AND ANALYSIS

In this section, global analyses are made with CDCC for neutron and proton scattering from ^{6,7}Li at $E \leqslant 150$ MeV. Particularly, we analyze the neutron total cross sections $\sigma_{\rm tot}$, the proton reaction cross sections $\sigma_{\rm R}$, and the differential cross sections for nucleon elastic and inelastic scattering from ^{6,7}Li.

A. Energy dependence of normalization factors

We determine the normalization factors, λ_V and λ_W, of the JLM effective NN interaction by fitting measured neutron total cross sections and proton reaction cross sections. The proton reaction cross sections are sensitive to λ_W, while the neutron total cross sections are to both λ_V and λ_W. This means that λ_V and λ_W can be determined uniquely from the two cross sections for each target of ^{6,7}Li.

Measured proton reaction cross sections [23] are not sufficient enough to determine the energy dependence of λ_V and λ_W up to 150 MeV. We then scale the measured reaction cross sections $\sigma_{\rm R}^{\rm exp}$ [24–27] for ^{9}Be target to the corresponding ones $\sigma_{\rm R}^{\rm scaled}$ for ^{6,7}Li targets, assuming that the reaction cross section is proportional to the effective collision area [28]. The scaling formula is expressed as [7]

$$\sigma_{\rm R}^{\rm scaled}({\rm Li}) = \frac{\sigma_{\rm R}^{\rm emp}({\rm Li})}{\sigma_{\rm R}^{\rm emp}(^9{\rm Be})}\sigma_{\rm R}^{\rm exp}(^9{\rm Be}), \tag{22}$$

where $\sigma_{\rm R}^{\rm emp}$ is the reaction cross section estimated from the effective collision area and depends on target mass number.

First we consider the case of ^{6}Li target. Figures 2 and 3 show the neutron total cross section and proton reaction cross section as a function of incident energy E, respectively. The normalization factors, λ_V and λ_W, are determined by fitting the measured cross sections [23–27,29]. The solid lines represent the CDCC results calculated with the optimal values of λ_V and λ_W, which are in good agreement with the measured cross sections. The factors thus determined are

$$\lambda_V(E) = 1 + 0.0035E,$$
$$\lambda_W(E) = \begin{cases} 0.015E & E \leqslant 30 \\ 0.45 + 0.0075(E-30) & E \geqslant 30 \end{cases}. \tag{23}$$

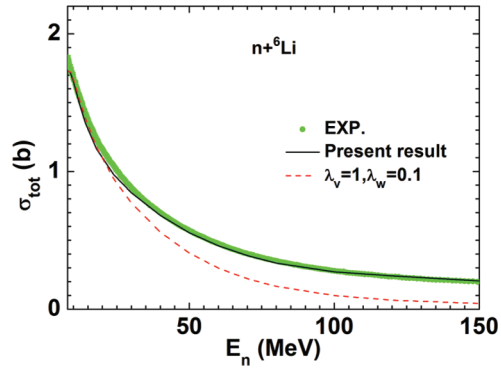

FIG. 2. (Color online) Comparison of the calculated total cross section for $n + {}^6$Li reaction with experimental data [29]. The solid and dashed lines denote the CDCC result with the normalization factors λ_V and λ_W determined in this work and that with $\lambda_V = 1$ and $\lambda_W = 0.1$, respectively.

The real part λ_V has a weak E dependence. The imaginary part λ_W is quite small at low E. This indicates that nucleon scattering at low E are well described by the CDCC formalism with the elastic, inelastic and breakup channels, i.e., excitations of d and α in target ^{6}Li are negligible. As E increases, the excitations do not keep negligible in general, and eventually λ_W becomes large there. This means that the ^{6}Li breakup into $n + p + \alpha$ channel is also considered roughly by λ_W. The dashed line in Fig. 2 shows the CDCC results calculated with $\lambda_V = 1$ and $\lambda_W = 0.1$ used in Ref. [12] for $n + {}^6$Li reaction at $E \leqslant 24$ MeV. Above 24 MeV, the dashed line deviates considerably from the corresponding measured cross sections. Therefore, the E dependence of λ_V and λ_W is significant above 24 MeV.

Similar analysis is made for ^{7}Li target. The optimal values of the normalization factors are expressed as

$$\lambda_V(E) = 1 + 0.0035E,$$
$$\lambda_W(E) = \begin{cases} 0.012E & E \leqslant 30 \\ 0.36 + 0.0075(E-30) & E \geqslant 30 \end{cases}. \tag{24}$$

The real part is the same as in the ^{6}Li case, while the imaginary part is slightly smaller than the one in the ^{6}Li case. This

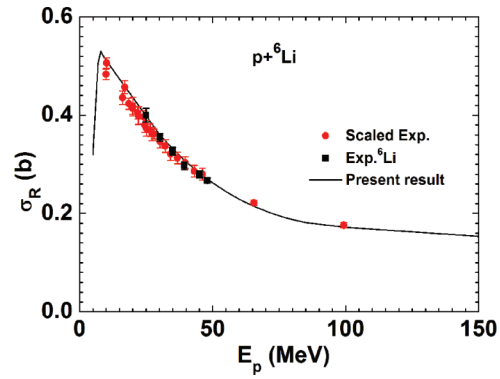

FIG. 3. (Color online) Comparison of the calculated result (solid line) of reaction cross section for $p + {}^6$Li reaction with experimental data [23–27]. The solid squares and circles denote the experimental data on $p + {}^6$Li reaction and the scaled experimental data transformed from $p + {}^9$Be reaction.

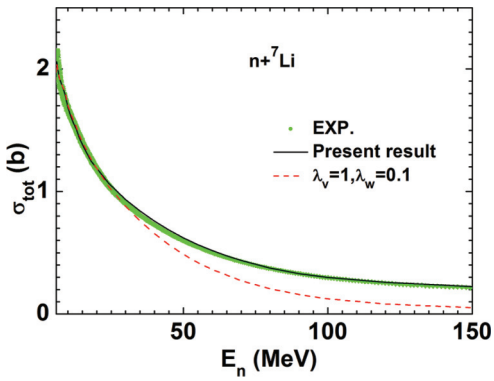

FIG. 4. (Color online) Same as Fig. 2 but for $n + {}^{7}$Li reaction.

is natural, since t in ^{7}Li is harder than d in ^{6}Li; note that the imaginary part comes from excitations of t and α for a ^{7}Li target and excitations of d and α for a ^{6}Li target. Figures 4 and 5 show the comparisons of the calculated results and experimental data [23–27,29] of the neutron total cross section and proton reaction cross section for ^{7}Li at incident energies up to 150 MeV. The solid lines denote the present results calculated with the normalization factors in Eq. (24). They are in good agreement with the experimental data. The dashed line in Fig. 4 shows the calculated results with $\lambda_V = 1$ and $\lambda_W = 0.1$ used in Ref. [14] for $n + {}^{7}$Li reaction at $E \leqslant 24$ MeV. Above 24 MeV, the dashed line deviates considerably from the corresponding measured cross section, which suggests that the energy dependence of the normalization factors given by Eq. (24) is necessary.

B. Nucleon elastic scattering

CDCC calculations with the normalization factors determined in Sec. III A are applied to the angular distributions for nucleon elastic scattering from ^{6,7}Li.

First we discuss the case of ^{6}Li target. Figure 6 shows the angular distributions of proton elastic scattering from ^{6}Li at incident energies of 5 MeV $\leqslant E \leqslant$ 72 MeV. CDCC results (solid lines) are in reasonable agreement with the experimental data [30–35]. The dashed lines represent results of the single elastic-channel calculation in which the couplings of the elastic channel to the breakup channels are ignored. Large deviation of the dashed lines from the solid ones indicates that the breakup effect is quite important.

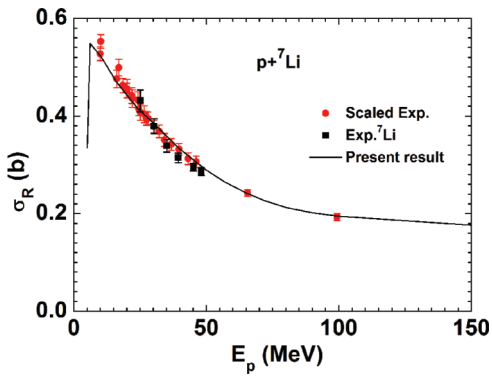

FIG. 5. (Color online) Same as Fig. 3 but for $p + {}^{7}$Li reaction.

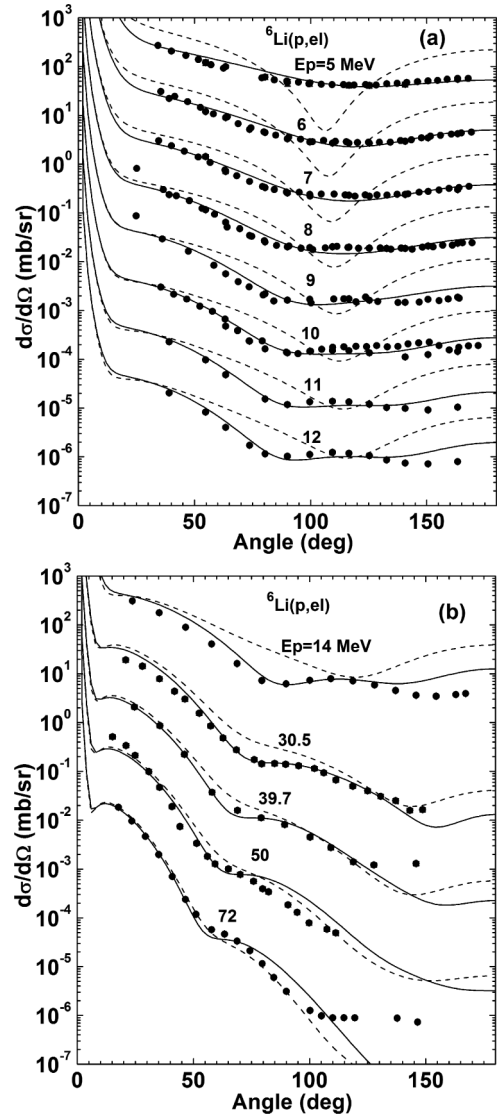

FIG. 6. Comparison of the calculated angular distributions (solid lines) of proton elastic scattering from ^{6}Li with experimental data [30–35]. The solid and dashed lines denote the CDCC results and the results of the single elastic-channel calculation, respectively. The data are shifted downward by factors of 10^{0}, 10^{-1}, 10^{-2}, and so on.

Figure 7 shows the angular distributions of neutron elastic scattering from ^{6}Li at 5.05 MeV $\leqslant E \leqslant$ 24 MeV. CDCC results (solid lines) are in good agreement with the experimental data [36–41]. The present CDCC results almost agree with the previous CDCC results [12] calculated with $\lambda_V = 1$ and $\lambda_W = 0.1$, and the difference between the two calculations is within 10%. The breakup effect is important also for $n + {}^{6}$Li elastic scattering.

Next we consider the case of ^{7}Li target. Figure 8 shows the angular distributions of proton elastic scattering from ^{7}Li at incident energies of 5 MeV $\leqslant E \leqslant$ 50 MeV. CDCC results (solid lines) reproduce the experimental data [32–34,42] well. ^{7}Li has two bound states, the ground state with $I^{\pi} = 3/2^{-}$ and the first-excited state with $\epsilon_1 = 0.48$ MeV and $I^{\pi} = 1/2^{-}$. In Fig. 9, we show the relative importance of couplings to the first-excited state and the continuum states. The solid lines

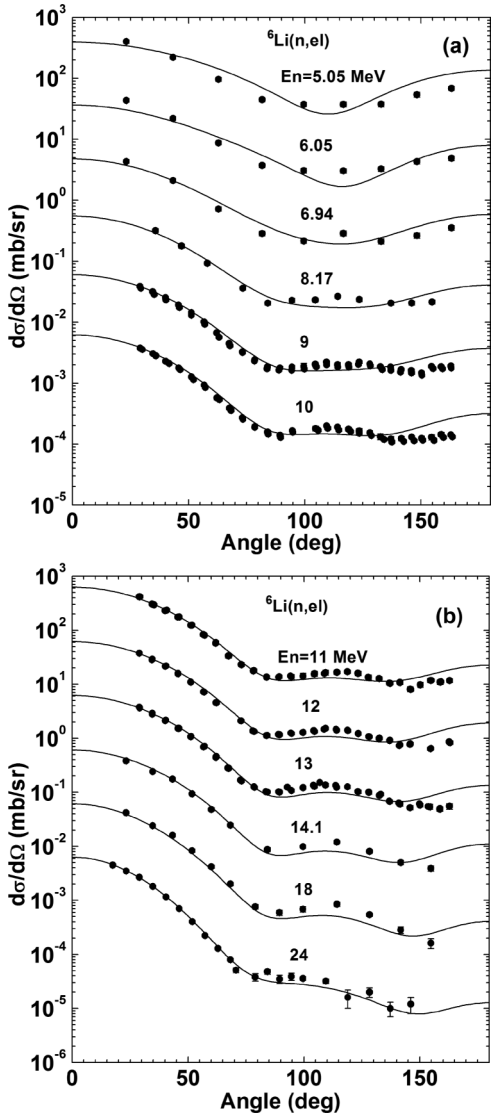

FIG. 7. Comparison of the calculated angular distributions (solid lines) of neutron elastic scattering from ^{6}Li with experimental data [36–41]. The data are shifted downward by factors of 10^0, 10^{-1}, 10^{-2}, and so on.

denote results of full-fledged CDCC calculations in which all the couplings are considered. The dotted lines represent CDCC calculations including only the coupling between the elastic and the first-excited channel, while the dashed lines denote results of single elastic-channel calculations with no coupling to the first-excited and continuum states. The difference between the dotted and dashed lines shows the effect of the coupling to first-excited state. Although it can slightly improve the results of the dashed lines, the results are still far from reproducing the experimental data. However, once the breakup effect shown by the difference between the solid and dotted lines is taken into account, the calculated results (solid lines) can reproduce the experimental data reasonably well. This indicates that the breakup effect is quite important in proton elastic scattering from ^{7}Li. In addition, it can be seen from Figs. 6 and 9 that the breakup effect becomes small as the incident energy increases. This is a general property of the breakup effect [3].

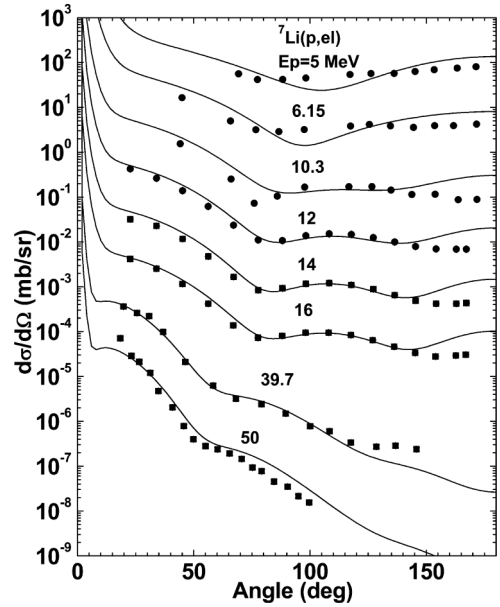

FIG. 8. Comparison of the calculated angular distributions (solid lines) of proton elastic scattering from ^{7}Li with experimental data [32–34,42]. The data are shifted downward by factors of 10^0, 10^{-1}, 10^{-2}, and so on.

Experimental data [39,43] on the angular distributions of neutron elastic scattering from ^{7}Li include the contribution from the inelastic scattering to the first-excited state, because of the poor experimental resolution. Summation of the calculated elastic and first inelastic scattering angular distributions are compared with the experimental data at 4 MeV $\leqslant E \leqslant$

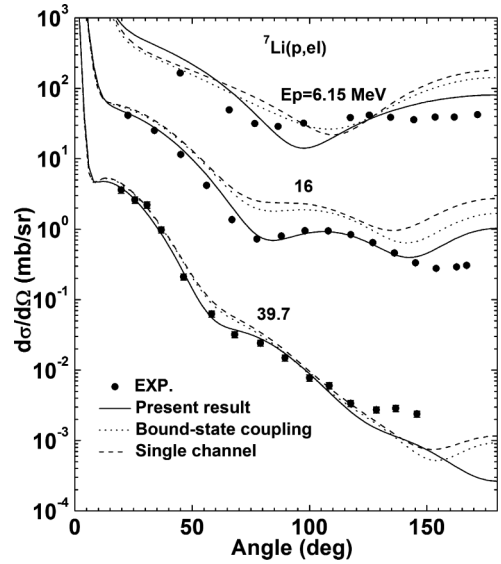

FIG. 9. Comparison of calculated angular distributions of proton elastic scattering from ^{7}Li with different couplings and experimental data. The solid lines denote the present calculated results with full CDCC. The dotted lines denote the coupled-channel calculation with the coupling only between the elastic and the first-excited channels. The dashed lines denote the results of the single elastic-channel calculation. The data are shifted downward by factors of 10^0, 10^{-1}, and 10^{-2}.

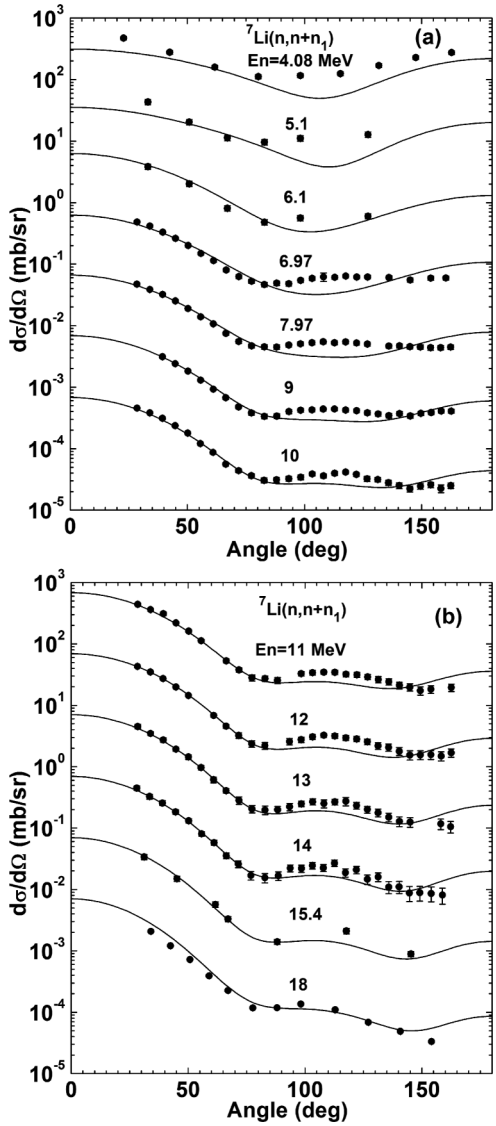

FIG. 10. Comparison of the calculated results (solid lines) of the summation of differential cross sections for neutron elastic and inelastic (the first $1/2^-$) scattering from ^{7}Li with experimental data [39,43]. The data are shifted downward by factors of 10^0, 10^{-1}, 10^{-2}, and so on.

18 MeV in Fig. 10. The calculated results (solid lines) are in reasonable agreement with the experimental data. The breakup effect is important also for $n + {}^7$Li elastic scattering.

C. Contribution of compound processes in elastic scattering

We analyze the effect of compound processes in elastic and inelastic scattering by using the Hauser-Feshbach theory with the width fluctuation correction. Figure 11 shows the differential cross sections for nucleon elastic scattering from ^{6,7}Li around $E = 5$ MeV. The solid and dashed lines represent CDCC results with and without compound contribution, respectively. The compound contribution, shown by the difference between the solid and dashed lines, is small and only seen around minima of the differential cross sections. The

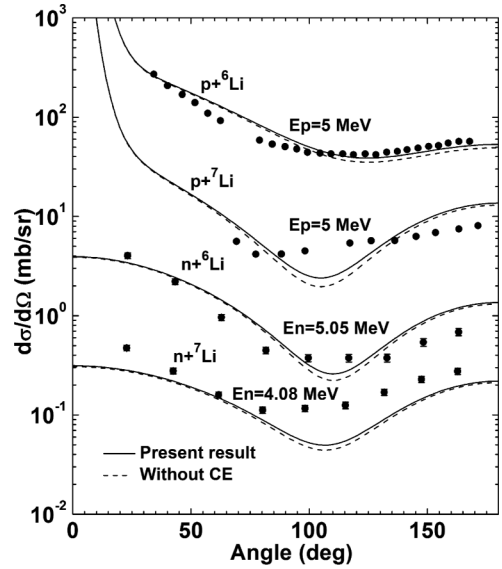

FIG. 11. Comparison of the calculated angular distributions of nucleon elastic scattering from ^{6,7}Li with and without the compound elastic scattering contribution. The solid and dashed lines denote the calculated results with and without the compound elastic contribution, respectively. The data are shifted downward by factors of 10^0, 10^{-1}, 10^{-2}, and 10^{-3}.

compound contribution decreases as E increases and become negligible at $E \geqslant 14$ MeV.

D. Nucleon inelastic scattering

Figure 12 shows the angular distributions of proton inelastic scattering to the first-excited state (3^+) of ^{6}Li at 4 MeV $\leqslant E \leqslant$ 14 MeV. The theoretical result is obtained by summing the inelastic cross sections to 3^+ continuum states

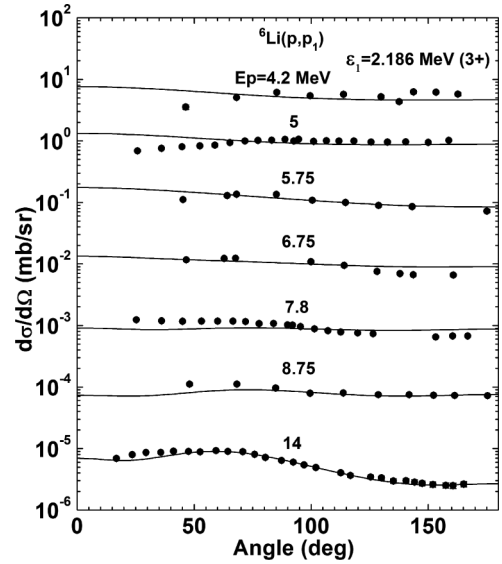

FIG. 12. Comparison of the calculated angular distribution (solid lines) of the proton inelastic scattering to the first-excited state (3^+) of ^{6}Li with experimental data [44,45]. The data are shifted downward by factors of 10^0, 10^{-1}, 10^{-2}, and so on.

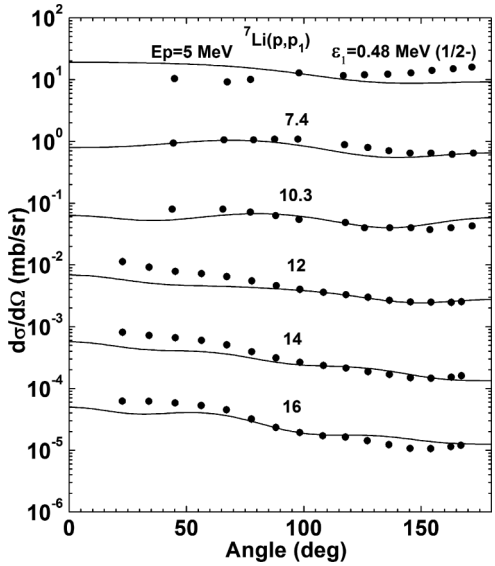

FIG. 13. Same as Fig. 12 but to the first-excited state $(1/2^-)$ of ^{7}Li.

in the resonance energy region. This summation can be easily made in the pseudostate method, since the continuum states in the resonance region are described by a few discretized states. CDCC results (solid lines) reproduce the experimental data [44,45] reasonably well for all the incident energies.

Figure 13 shows angular distributions of proton inelastic scattering to the first-excited state $(1/2^-)$ of ^{7}Li at 5 MeV $\leqslant E \leqslant$ 16 MeV. CDCC results (solid lines) are consistent with the experimental data [32,42,46]. Agreement becomes worse slightly at forward angles for the cases of $E = 12$, 14 and 16 MeV. Similar comparisons are made for neutron inelastic scattering to the first-excited state (3^+) of

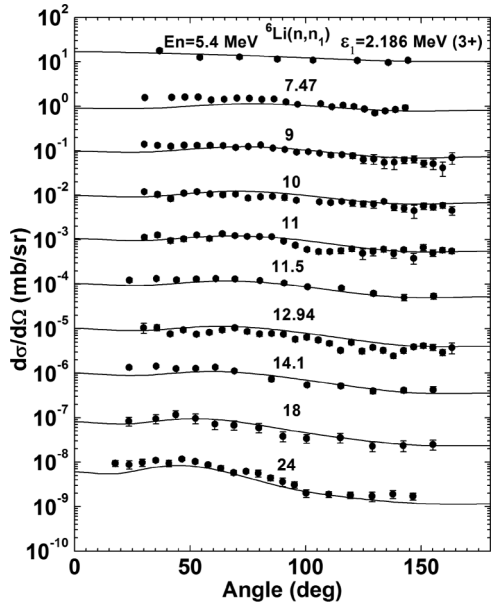

FIG. 14. Comparison of the calculated angular distribution (solid lines) of the neutron inelastic scattering to the first-excited state (3^+) of ^{6}Li with experimental data [37–39,45]. The data are shifted downward by factors of 10^0, 10^{-1}, 10^{-2}, and so on.

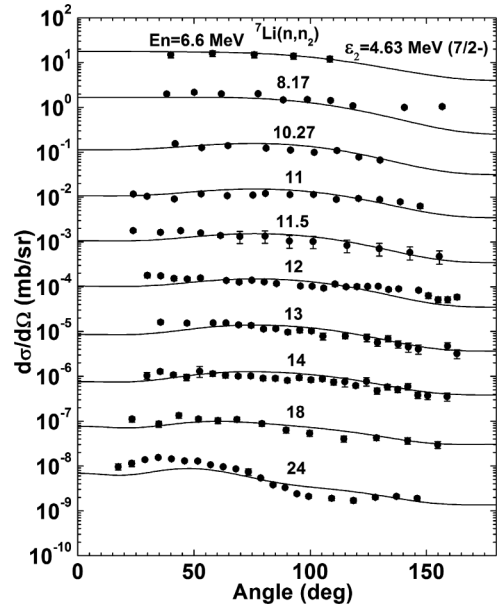

FIG. 15. Same as Fig. 14 but to the second-excited state $(7/2^-)$ of ^{7}Li.

^{6}Li at incident energies from 5.4 to 24 MeV in Fig. 14, and neutron inelastic scattering to the second-excited state $(7/2^-)$ of ^{7}Li at incident energies from 6.6 to 24 MeV in Fig. 15. The experimental data are taken from Refs. [37,39–41,43,47–49]. Rather good agreement is obtained for these cases. The compound inelastic scattering contributions are also included in all the calculations, resulting in improvement of pure CDCC results by at most 10% at relatively low energies.

IV. SUMMARY AND CONCLUSION

We have analyzed systematically nucleon scattering from ^{6,7}Li at incident energies up to 150 MeV by using the continuum discretized coupled channels method (CDCC) with the Jeukenne-Lejeune-Mahaux (JLM) interaction. Energy dependence of the normalization factors, λ_V and λ_W, of the JLM interaction is introduced and determined explicitly from measured neutron total and proton reaction cross sections. The real part λ_V has no target dependence, while λ_W has a weak one. The compound elastic and inelastic scattering components have been calculated by using the Hauser-Feshbach theory with the width fluctuation correction. The compound contribution slightly improves CDCC results at low incident energies. In most cases, CDCC results are in good agreement with the experimental data on angular distributions of nucleon elastic and inelastic scattering from ^{6,7}Li. It is essential to take into account the breakup effect of ^{6,7}Li properly with CDCC in order to describe both the elastic and inelastic scattering consistently. Good agreement of CDCC results with experimental data shows the rationality of the determined normalization factors of the JLM interaction, and the importance of the breakup effect of ^{6,7}Li indicates the necessity of CDCC for systematic analyses of nucleon scattering from ^{6,7}Li over a wide range of incident energies.

Double-differential cross sections (DDXs) of secondary nucleon and triton produced in these reactions are also very

important physical quantities in the engineering design of D-T fusion reactors and intense neutron sources with a lithium target. The present CDCC analysis has confirmed the importance of breakup effect and has provided a good basis for predicting these DDXs. In the next step, the production of secondary nucleon and triton will be studied intensively with CDCC.

ACKNOWLEDGMENTS

We would like to thank Satoshi Chiba for helpful discussions and comments. This work was supported by Grant-in-Aid for Scientific Research of the Japan Society for the Promotion of Science (Grant No. 22560820).

[1] P. Garin and M. Sugimoto, J. Nucl. Mater. **417**, 1262 (2011), and references therein.
[2] R. A. Forrest, R. Capote, N. Otsuka, T. Kawano, A. J. Koning, S. Kunieda, J-Ch. Sublet, and Y. Watanabe, FENDL-3 Library, Summary documentation, INDC(NDS)-0628, International Atomic Energy Agency (2012).
[3] M. Kamimura, M. Yahiro, Y. Iseri, Y. Sakuragi, H. Kameyama, and M. Kawai, Prog. Theor. Phys. Suppl. **89**, 1 (1986).
[4] N. Austern, Y. Iseri, M. Kamimura, M. Kawai, G. Rawitscher, and M. Yahiro, Phys. Rep. **154**, 125 (1987).
[5] M. Yahiro, K. Ogata, T. Matsumoto, and K. Minomo, Prog. Theor. Exp. Phys. (2012) 01A206.
[6] Y. Sakuragi, M. Yahiro, and M. Kamimura, Prog. Theor. Phys. **70**, 1047 (1983).
[7] T. Ye, Y. Watanabe, K. Ogata, and S. Chiba, Phys. Rev. C **78**, 024611 (2008).
[8] J. Lubian, T. Correa, E. F. Aguilera, L. F. Canto, A. Gomez-Camacho, E. M. Quiroz, and P. R. S. Gomes, Phys. Rev. C **79**, 064605 (2009).
[9] G. R. Kelly *et al.*, Phys. Rev. C **63**, 024601 (2000).
[10] K. Rusek, N. Alamanos, N. Keeley, V. Lapoux, and A. Pakou, Phys. Rev. C **70**, 014603 (2004).
[11] D. Ichinkhorloo, T. Matsumoto, Y. Hirabayashi, K. Katō, and S. Chiba, J. Nucl. Sci. Technol. **48**, 1357 (2011).
[12] T. Matsumoto, D. Ichinkhorloo, Y. Hirabayashi, K. Katō, and S. Chiba, Phys. Rev. C **83**, 064611 (2011).
[13] J. P. Jeukenne, A. Lejeune, and C. Mahaux, Phys. Rev. C **16**, 80 (1977).
[14] D. Ichinkhorloo, Y. Hirabayashi, K. Katō, M. Aikawa, T. Matsumoto, and S. Chiba, Phys. Rev. C **86**, 064604 (2012).
[15] A. M. Moro, J. M. Arias, J. Gomez-Camacho, I. Martel, F. Perez-Bernal, R. Crespo, and F. Nunes, Phys. Rev. C **65**, 011602 (2001).
[16] T. Matsumoto, T. Kamizato, K. Ogata, Y. Iseri, E. Hiyama, M. Kamimura, and M. Yahiro, Phys. Rev. C **68**, 064607 (2003).
[17] M. Kamimura, Phys. Rev. A **38**, 621 (1988).
[18] E. Hiyama, Y. Kino, and M. Kamimura, Prog. Part. Nucl. Phys. **51**, 223 (2003).
[19] S. Saito, Prog. Theor. Phys. **41**, 705 (1969).
[20] W. Hauser and H. Feshbach, Phys. Rev. **87**, 366 (1952).
[21] A. J. Koning, S. Hilaire, and M. C. Duijvestijn, in *Proceedings of the International Conference on Nuclear Data for Science and Technology, April 22–27, 2007, Nice, France*, edited by O. Bersillon, F. Gunsing, E. Bauge, R. Jacqmin, and S. Leray (EDP Sciences, Les Ulis, 2008), p. 211.
[22] A. J. Koning and J. P. Delaroche, Nucl. Phys. A **713**, 231 (2003).
[23] R. Carlson *et al.*, Nucl. Phys. A **445**, 57 (1985).
[24] W. Mcgill *et al.*, Phys. Rev. C **10**, 2237 (1974).
[25] P. Kirkby and W. Link, Can. J. Phys. **44**, 1847 (1966).
[26] A. Ingemarsson *et al.*, Nucl. Phys. A **653**, 341 (1999).
[27] B. Wilkins and G. Igo, Phys. Rev. **129**, 2198 (1963).
[28] H. Bradt and B. Peters, Phys. Rev. **77**, 54 (1950).
[29] W. P. Abfalterer, F. B. Bateman, F. S. Dietrich, R. W. Finlay, R. C. Haight, and G. L. Morgan, Phys. Rev. C **63**, 044608 (2001).
[30] M. Haller, M. Betz, W. Kretschmer, A. Rauscher, R. Schmitt, and W. Schuster, Nucl. Phys. A **496**, 189 (1989).
[31] W. Harrison and A. Whirehead, Phys. Rev. **132**, 2607 (1963).
[32] N. Koori, I. Kumabe, M. Hyakutake, K. Orito, K. Akagi, A. Iida, Y. Watanabe, K. Sagara, H. Nakamura, K. Maeda, T. Nakashima, M. Kamimura, and Y. Sakuragi, Japan Atomic Energy Research Institute Report No. JAERI-M 89-167, 1989 (unpublished).
[33] S. Chen and N. M. Hintz, in *International Conference on Nuclear Forces and the Few Nucleon Problem*, edited by T. C. Griffith and E. A. Power (Pergamon Press, New York, 1960), p. 683.
[34] G. Mani, A. Dix, D. Jones, and M. Richardson, Rutherford Laboratory Report No. RHEL/R-136, 1967 (unpublished), p. 49.
[35] R. Henneck, G. Masson, P. Eversheim, R. Gebel, F. Hinterberger, U. Lahr, H. Schmitt, J. Schleef, and B. Przewoski, Nucl. Phys. A **571**, 541 (1994).
[36] H. Knox, R. White, and R. Lane, Nucl. Sci. Eng. **69**, 223 (1979); EXFOR-10710 data file entry.
[37] X. Ruan *et al.*, High Energ. Phys. Nucl. Phys. **31**, 442 (2007); EXFOR-31605 data file entry.
[38] J. H. Dave and C. R. Gould, Phys. Rev. C **28**, 2212 (1983).
[39] H. Hogue *et al.*, Nucl. Sci. Eng. **69**, 22 (1979); EXFOR-10707 data file entry.
[40] S. Chiba *et al.*, Phys. Rev. C **58**, 2205 (1998).
[41] L. F. Hansen, J. Rapaport, X. Wang, F. A. Barrios, F. Petrovich, A. W. Carpenter, and M. J. Threapleton, Phys. Rev. C **38**, 525 (1988).
[42] K. Kilian, G. Clausnitzer, W. Durr, D. Fick, R. Fleischmann, and H. M. Hofmann, Nucl. Phys. A **126**, 529 (1969).
[43] M. Baba, N. Hayashi, T. Sakase, T. Iwasaki, S. Kamata, and T. Momota, Bull. Am. Phys. Soc. **24**, 862 (1979); EXFOR-21630 data file entry.
[44] W. Harrison, Nucl. Phys. A **92**, 253 (1967).
[45] F. Merchez, R. Bouchez, R. Hoffswell, and A. Yavin, J. Phys. **29**, 969 (1968).
[46] N. Koori, I. Kumabe, M. Hyakutake, Y. Watanabe, K. Orito, K. Akagi, A. Iida, M. Eriguchi, Y. Wakuta, K. Sagara, H. Nakamura, K. Maeda, and T. Nakashima, Japan Atomic Energy Research Institute Report No. JAERI-M 91-009, 1991 (unpublished).
[47] S. Chiba, M. Baba, H. Nakashima, M. Ono, N. Yabuta, S. Yukinori, and N. Hirakawa, J. Nucl. Sci. Technol. **22**, 771 (1985).
[48] S. Chiba, Y. Yamanouti, M. Mizumoto, M. Hyakutake, and S. Iwasaki, J. Nucl. Sci. Technol. **25**, 210 (1988).
[49] M. Ibaraki, M. Baba, S. Matsuyama, T. Sanami, T. Win, T. Miura, and N. Hirakawa, J. Nucl. Sci. Technol. **35**, 843 (1998).